
Cholesteric Liquid Crystal Flakes—A New Form of Domain

The last 20 years have seen a growth of mixed-media systems in which cholesteric liquid crystals (CLC's) are one component. These include polymer-dispersed CLC's¹ in which the CLC's are confined to microdroplets within a continuous isotropic polymer and CLC's in gels² in which there is a small amount of polymer to stabilize the CLC structure. In either case, the continuity of the cholesteric texture is interrupted.

CLC's are characterized by a structure in which the average direction of molecules in a given plane, indicated by a unit vector called the director \mathbf{n} , rotates about an axis. The continuously rotating director produces a helix. The length through which the director makes a complete 360° cycle is called the pitch P of the cholesteric. When the orientation of the helix axis is normal to the boundary surfaces, the texture produced is called Grandjean or planar.³ This texture is responsible for the selective wavelength and polarization reflection unique to CLC's.⁴ The center of the selective reflection wavelength band is given by

$$\lambda_0 = \bar{n}_n P, \quad (1)$$

where \bar{n}_n = the average refractive index at a given plane perpendicular to the helix, calculated⁵ from the ordinary and extraordinary cholesteric refractive indices.

The optical characterization of the CLC structure may be done by several methods. One of the simplest ways to evaluate the homogeneity of the Grandjean texture is with a polarizing microscope. A CLC sample aligned to the Grandjean texture is viewed between crossed polarizers. Dark areas indicate that the molecules through which the light has passed are either perfectly aligned with the polarizer or analyzer or isotropically distributed. In either case, for CLC's, dark spots and lines indicate deviations from cholesteric structure that are referred to as *disclinations*.^{6,7} Regions between the disclinations are called *domains*, although there is some lack of consensus about the physical nature of a domain. There is some sense of a discrete area in which the director orientation is essentially

constant, although this is usually subjectively determined by judging areas that appear homogeneous.^{8,9} The term *monodomain* refers to regions that can be characterized by a single director. When directors characterize domains that are rather random with respect to each other, the region is considered *polydomain*.¹⁰

While domain boundaries may exhibit clear-cut disclinations, domains may not always be separated by a well-defined surface. Instead, there may be a discontinuity in the director orientation.¹¹ These discontinuities were first observed by Grandjean¹² and correctly described by Cano¹³ as being caused by pitch deformations. The helix stretches or contracts to span the gap of the cell with an integer multiple of half-pitches. When the elastic limit is reached, the helix structure either inserts or removes a half-pitch. Although these discontinuities are called *Cano lines*, they do not actually appear as lines but as borders between regions differing in thickness by one half-pitch. Between crossed linear polarizers, this manifests as different retardances and therefore different colors.^{14,15}

Other imaging techniques, including scanning electron microscopy (SEM), transmission electron microscopy (TEM), and atomic force microscopy (AFM), have been developed to image the periodic structure of CLC's in the planar/Grandjean texture. For example, a sample of low-molecular-weight (LM) CLC was frozen between metal sheets, the sheets were forced apart, and platinum-carbon replicas of the resulting fractured edges were examined by SEM.^{16–18} Periodic striations corresponding to the half-pitch suggested that the fracturing occurred along the helix profile. Even disclinations could be viewed by this technique. Not only replicated samples but also the frozen CLC's themselves were examined using SEM.¹⁹ Because of LMCLC samples unfreezing or ice building up on the surfaces, DeGennes²⁰ suggested the use of polymerized CLC's for SEM study. This experiment was conducted for the first time in 1993²¹ to visualize the molecular distribution around a Cano line. The images showed that there were layers to the molecular distribution, but no additional quantitative analysis was done.

Atomic force microscopy, developed in 1985,²² has been used to examine Langmuir–Blodgett and transferred freely-suspended liquid crystal films²³ as well as liquid crystal films on graphite.²⁴ Liquid crystal films have shown some two-dimensional structure and some cholesteric periodicity but are often deformed by contact with the cantilever tip.

Cyclic polysiloxane oligomers,^{25,26} in particular, have been examined by Bunning *et al.*^{27,28} with TEM and AFM. Samples for these studies were aligned to the Grandjean texture by shearing between Teflon sheets, cooled to below their glass transition temperatures, and microtomed, producing samples free of the effect of underlying support²⁹ substrates. Results indicate that the cyclic polysiloxanes do show corrugated fresh surfaces with a periodicity equal to one-half the pitch. From TEM and AFM results, in conjunction with x-ray diffraction studies, Bunning *et al.*^{30,31} drew further conclusions regarding the structural morphology. Their proposed structure consists of interdigitated sidechains, the extent of association being dependent on the composition and temperature. The siloxane backbones form layers that twist into the helical structure of the cholesteric with the sidechains aligned along the director \mathbf{n} .

Imaging the multiple domains of the CLC's within mixed-media systems by the techniques described above is complicated by the production methods of these mixed-media systems. Methods include (a) emulsification³² of the liquid crystal with a polymer and (b) phase separation³³ of the liquid crystal from solution with a polymer. The CLC domains are produced at the same time as the mixed medium itself. As a result, the domains can be characterized only *within* the medium. The domains may be diluted or contaminated by other components of the mixture.³⁴ Polymer “walls” may affect molecular alignment at domain boundaries.³⁵

In this article, we describe the production and characterization of a new form of CLC's called *flakes*, proposed by Faris.³⁶ We examine individual flakes by optical light microscopy, SEM, and AFM. We will show that flakes maintain many of the optical properties of the continuous films from which they are made. The CLC flakes can be embedded into a host to form a new type of mixed medium in which the flakes provide well-characterized CLC domains. We will show how the orientation of these CLC flakes can be evaluated quantitatively using Bragg's Law in the form of Ferguson's Equation:³⁷

$$\lambda_r = \lambda_0 \cos \left\{ \frac{1}{2} \left[\sin^{-1} \left(\frac{\sin \theta_i}{\bar{n}_{\text{ch}}} \right) + \sin^{-1} \left(\frac{\sin \theta_r}{\bar{n}_{\text{ch}}} \right) \right] \right\}, \quad (2)$$

where λ_0 = the wavelength at the center of the selective reflection band at normal incidence, λ_r = the wavelength at the center of the selective reflection band at oblique incidence, θ_i = incidence angle, θ_r = observation angle in air, and \bar{n}_{ch} = the approximate average cholesteric refractive index.

The orientation of CLC flakes can be further understood by using a function known as turbidity τ . This useful parameter has been developed³⁸ for nematic droplets dispersed in a matrix that does not absorb liquid crystal. It characterizes the extent of scattering as a function of incidence angle and refractive index mismatch in the anomalous diffraction regime. Turbidity has not yet been investigated for cholesteric materials, but for nematics has been defined as

$$\tau = -\ln \left[\frac{T_{\text{sample}}(\theta_i)}{T_{\text{blank}}(\theta_i)} \right] \frac{\cos[\sin^{-1}(\sin \theta_i / n_{\text{med}})]}{t}, \quad (3)$$

where $T_{\text{sample}}(\theta_i)$ = transmittance of a sample, $T_{\text{blank}}(\theta_i)$ = transmittance of a blank used to correct for reflection from the film and substrate, t = thickness of the sample, and n_{med} = the refractive index of the embedding medium.

Preparation of CLC Flakes

Two types of cyclic polysiloxanes were used in this study: (a) noncrosslinkable of the type shown in Fig. 74.73 (adapted from Ref. 26), obtained from Wacker–Chemie in Munich³⁹ and designated CLC670, which refers to its λ_0 in nm and (b) crosslinkable, designated CC3767 and similar to that of Fig. 74.73 but with terminal methacryl groups and crosslinked by UV curing in the presence of a photoinitiator.⁴⁰ The exact ratios of chiral to nonchiral side-chains and the amount of added monomer (to reduce viscosity for ease of workability) are proprietary to the manufacturer.

In a procedure referred to as “knife-coating,” the noncrosslinkable material is applied onto a silicon wafer,⁴¹ which is heated to 130°C on a hotplate;⁴² polysiloxane is then melted onto the substrate surface. A microscope slide placed on edge and referred to as the “knife” is used to smear the polysiloxane across the surface. This knife-coating process causes the CLC to be aligned in the Grandjean texture as observed by reflective color. The substrate is then quickly removed from the hotplate, allowing the CLC to be quenched to room temperature, “freezing in” the helical structure of the Grandjean texture. The CLC films prepared in this way are ~30 μm thick.

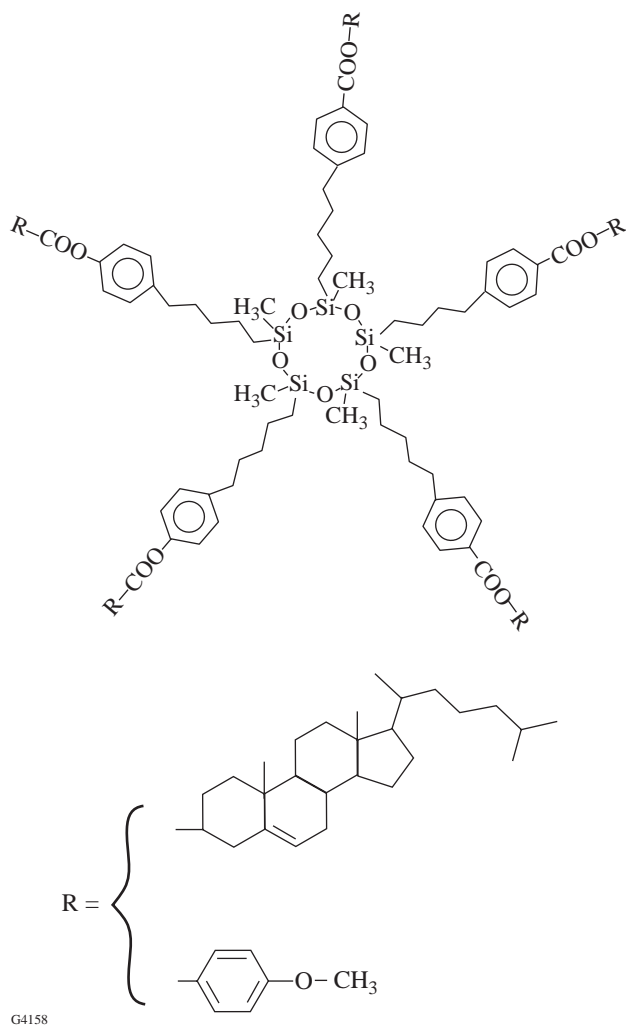


Figure 74.73
Structure of cyclic polysiloxane used in this study.

The crosslinked material is prepared by mixing the CLC with photoinitiator (1.5% by weight), sprinkling in 13- μm -sized glass fiber spacers,⁴³ and shearing the mixture between two 3-cm-diam, fused-silica substrates at 100°C. The sandwich cell, still at 100°C, is exposed for 2 min to ultraviolet light of $\lambda = 365 \text{ nm}$ and 15 mW/cm^2 at 5-cm distance.⁴⁴ After curing, the cell is pried open with a razor blade to expose the cured film.

For either method of preparation, the resulting “open-faced” film is placed in a Petri dish and covered with liquid nitrogen. The polymer CLC fractures and lifts slightly and temporarily off the silicon or glass surface. Methanol is used to wash the fractured CLC off the substrate.

Imaging Individual Flakes

1. Light Microscope

Viewed under a light microscope, flakes appear to be irregularly shaped with sharp corners. Figure 74.74 shows a micrograph of CLC670 flakes between crossed polarizers.⁴⁵ All samples show similar features. The flakes themselves appear to have few disclinations or Cano lines, suggesting that fracturing occurred along disclinations and discontinuities in the film, consistent with theoretical freeze-fracture models.¹⁷

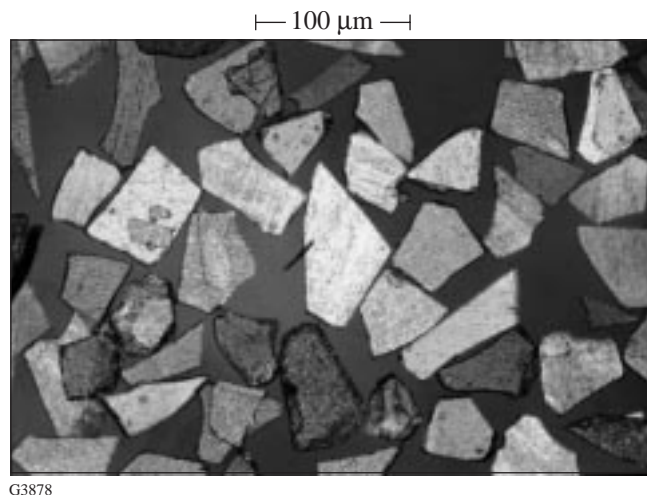


Figure 74.74
Photomicrograph of CLC670 flakes.

2. Scanning Electron Microscope

CC3767 (crosslinked) flakes were sputtered with silver and examined using scanning electron microscopy.⁴⁶ Samples like the one in Fig. 74.75 are seen to have an even more irregular structure than that which appeared under light microscopy. Some swelling is apparent at the edges of the flakes, which we attribute to absorption of the methanol used for the slurry. Periodic ridges are evident on many of the flakes. The freeze-fracture process appears to occur along the cholesteric helix profile, perpendicular to the director. From rough estimation of the magnitude of the pitch measured physically on the SEM observation screen, the pitch appears to be 486 nm. Based on Eq. (1) and prefracture measurements of $\lambda_0 (= 712 \text{ nm})$ and $\bar{n}_n (= 1.5812 \text{ at } 712 \text{ nm})$, the optically calculated pitch for this sample is 450 nm. The similar magnitude of the numbers suggests that the observed periodic ridges are, in fact, indicative of pitch. Due to parallax caused by the tilt of the sample and the SEM sample table, however, measurements from these photographs are only estimates.

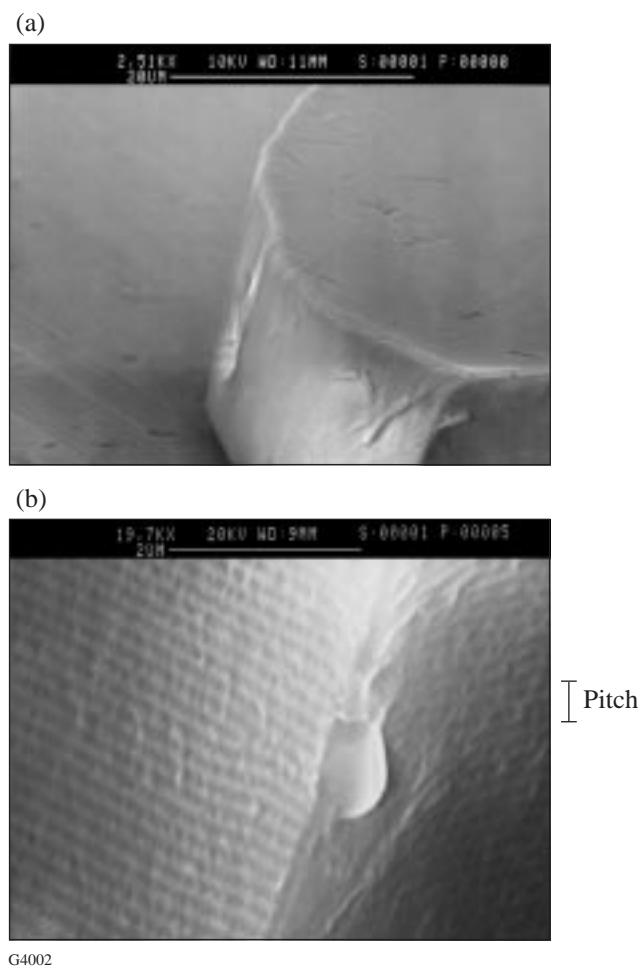


Figure 74.75 Scanning electron micrographs of a CLC flake (sample: CC3767). (a) There is slight swelling at the edges of a flake. (b) At higher magnification, periodic ridges corresponding to the pitch can be seen.

The noncrosslinked flakes were also examined with SEM. These also showed ridges consistent with half-pitch periodicity. Neither sputtering nor SEM voltage appeared to damage, melt, or decompose any of the flakes.

3. Atomic Force Microscope

To determine pitch physically and without parallax, a single CC3767 flake was mounted vertically against a small piece of glass using epoxy.⁴⁷ The flake was placed in an atomic force microscope⁴⁸ whose tip consisted of a pyramidal crystal of silicon nitride attached to a cantilever. The edge of the flake was rastered under this cantilever. Deflections of the cantilever by the surface resulted in an image profile of the surface like the one shown in Fig. 74.76. Our images are consistent with the microtomed and free-surface AFM images of chol-

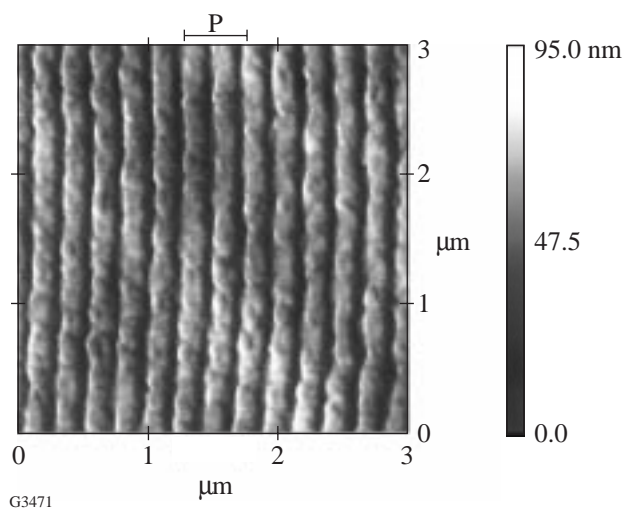


Figure 74.76 Atomic force micrograph of a CLC flake edge (sample: CC3767). The pitch measured from this image is 451 nm.

estic polysiloxanes obtained by Meister *et al.*⁴⁹ and provide a third unique view of the cholesteric corrugation due to pitch periodicity.

Since there is no parallax in this image, the pitch can be measured directly to be 451 nm. The pitch calculated from the prefracture optical measurements, listed in the **Scanning Electron Microscope** section, is 450 nm. The excellent agreement confirms that the ridges seen in both SEM and AFM images are those of the cholesteric helix profile exposed by freeze-fracturing. More importantly, the process of producing flakes from polymer CLC films maintains the pitch and, as we will show, the selective wavelength reflection capability of the original film.

AFM measurements of the noncrosslinkable CLC670 gave equally good agreement of physically measured and optically calculated pitch. The remaining tests described below used only the noncrosslinkable material to avoid the time-consuming process of preparing, curing, and splitting sandwich cells.

Sizing of CLC Flakes

To separate flakes by size, a stack of stainless steel screen sieves⁵⁰ is used. Table 74.V lists the mesh sizes and nominal particle-size ranges when stacked in order of increasing mesh number. Flakes in methanol slurry are dripped into the sieve stack, using methanol to wash the flakes through. Each stage is washed with methanol until the effluent appears visually clear. Material retained by each sieve is collected by methanol slurry and allowed to dry by evaporation. For a typical initial charge

Table 74.V: Sieve designations and measured ranges of CLC670 flakes.

| Sieve designation (mesh size) | Nominal particle-size range (μm) that should be trapped in sieve | Median and standard deviation of each sieve group of CLC670 flakes measured by Horiba LA-900 (μm) |
|-------------------------------|---|--|
| 80 | >180 | 218±204 |
| 170 | 90–180 | 124±28 |
| 325 | 45–90 | 66±26 |
| 635 | 20–45 | 35±16 |
| Pan | <20 | 24±14 |

of about 5 g of flakes, the sieving process typically requires about 5 h to completely separate the larger-sized flakes (>45 μm) into three groups. The “20- to 45- μm ” sieve cut takes an additional 4 h of sieving time. All separated samples are allowed to dry for 4 days.

To test whether the sieve separation technique was efficient, each sieve cut (what was trapped in the sieve as well as the final bottom collection pan) was tested for particle-size distribution using the Horiba LA-900 Particle Analyzer.⁵¹ In this instrument, the particles are suspended in a fluid. For the CLC flakes, this fluid was methanol. No additional surfactant was used since initial testing with detergent as a surfactant led to the formation of bubbles, which interfered with particle detection. A small-fraction sample container of approximately 50-mL volume was used. In the small-fraction container, particles were kept in suspension in the instrument’s light beam using a magnetic stirrer. The particles scattered and diffracted light from both a HeNe laser beam and a beam from a halogen lamp. The latter was equipped with two filters: one to pass 610-nm light and one to pass 480-nm light. Size distribution was determined based on an instrument algorithm that calculates the distribution of spherical particles that would give the same scattering pattern as the sample particles. The distribution of the algorithm’s spherical particles is given as a percent frequency F%. The size range detectable by the Horiba LA-900 is 0.04 to 1000 μm . Plots are typically Gaussian in shape on a semilogarithmic scale for a natural distribution of particles.⁵² For particles that are not uniform in shape, such as the CLC flakes, the particle analyzer detects the largest dimension,⁵³ so the median value of such a distribution lies on the high side of the sieve designation. The measured results are shown in Table 74.V.

Each size-group of CLC670 is plotted in Fig. 74.77 to show if the different size-group distributions are well or poorly

separated. The vertical lines indicate the nominal ranges based on the sieve designations listed in Table 74.V. The medians and modes are well separated. In general, however, the “>180- μm ” group contains flakes that exceed the Horiba LA-900 size-detection limits. The “<20- μm ” group shows some agglomeration. Otherwise, each mode falls within the sieve-size designation. There is overlap among the groups within the standard deviations for each distribution, so we may expect to see trends in optical behavior related to size but probably no optical behavior unique to a particular size-group since each group contains some flakes whose sizes are common to adjacent groups.

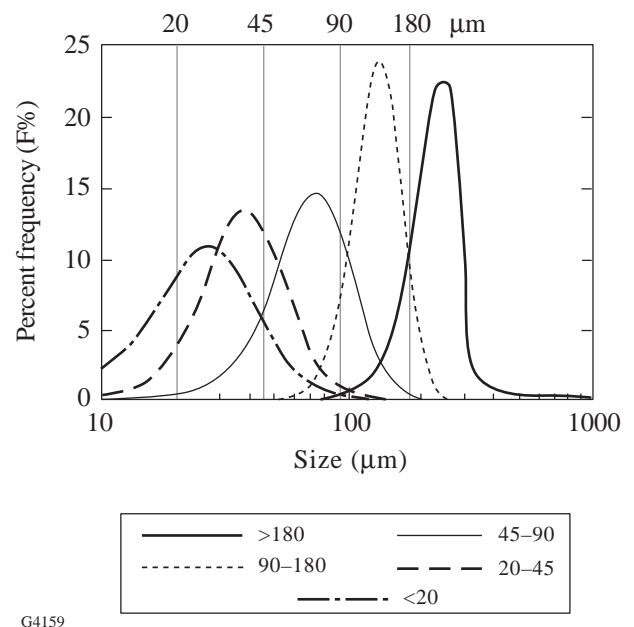


Figure 74.77 Effectiveness of sieving for separating size-groups. The vertical lines indicate the nominal size limits of the sieve designations.

Orientation of CLC Flakes

Glass disk substrates made from a conveniently available float glass ($n_{D,20} = 1.533$, 25-mm diameter, 1 mm thick) were weighed; then 1 mL of deionized water was dropped by graduated pipet onto each substrate to cover it to the edge. Flakes in methanol slurry were dripped onto the water bead by a medicine dropper. The flakes oriented themselves with their largest surface parallel to the meniscus. When the surface was visually covered with flakes, the underlying fluid was removed by medicine dropper. Each sample was allowed to dry. At regular intervals, each sample was weighed until three identical readings were obtained, indicating that the samples had completely dried (about 48 h total). After all the optical tests were completed for a given sample, its thickness was measured by contact gauge⁵⁴ in five spots and averaged. The gauge tip tended to disturb the flakes, so thickness measurements could not be made until optical testing was completed.

Since the $>180\text{-}\mu\text{m}$ and $<20\text{-}\mu\text{m}$ sieve groups for CLC670 were of anomalous size, they were excluded from optical testing so that comparisons of size effects on optical behavior could be drawn with more certainty by being based on the other three sieve groups. In addition, the $>180\text{-}\mu\text{m}$ flakes, when oriented by water bead, did not completely cover the substrate. The $<20\text{-}\mu\text{m}$ flakes, when oriented by water bead, tended to aggregate into visually observable inhomogeneities. Therefore, even qualitative comparisons involving these extreme sizes were not feasible.

Selective Reflection

Transmittance profiles of each size-group were determined by spectrophotometer⁵⁵ at 0° incidence. The results of three size-groups are shown in Fig. 74.78. There is a dramatic drop in overall transmittance with decreasing flake size; however, each size-group continues to show the selective wavelength reflection (manifested by a transmittance valley) characteristic of CLC's.

In addition, a CLC670 “45- to $90\text{-}\mu\text{m}$ ” sample prepared by water-bead orientation was examined in transmission using right-hand circular and then left-hand circular incident polarization. Figure 74.79 shows that the CLC flakes continue to exhibit the selective polarization-handedness reflectivity also characteristic of CLC's.

Clearly, we have discrete CLC domains of prealigned Grandjean texture that continue to exhibit the selective wavelength and polarization of unfractured CLC films or of CLC polymer-dispersed or gel systems. These domains, however,

are uncontaminated by any processing steps. The CLC flakes are also not subject to the alignment deformities that might be caused by confining walls.

The additional optical tests performed on these CLC flake samples will allow us to make comparisons by flake-size of orientation quality. In particular, we will look at the angle dependence of both the selective reflection wavelength and the scattering, considering CLC flakes as distributions of discrete cholesteric domains.

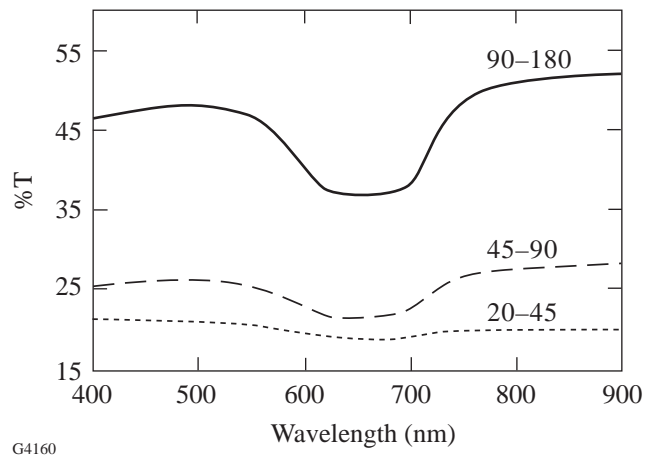


Figure 74.78
Transmittance profiles of three sieve groups.

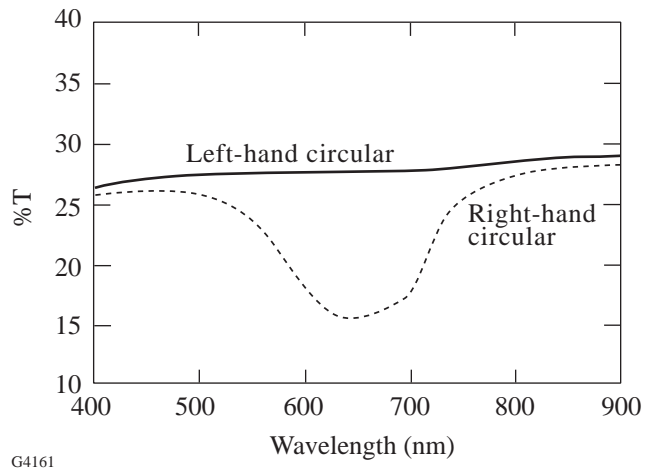
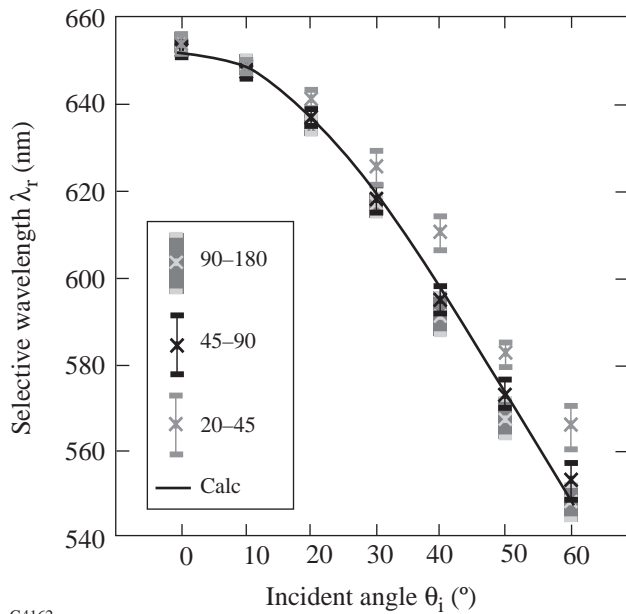


Figure 74.79
Selective polarization handedness of CLC flakes.

Angle Dependence of Selective Wavelength

Three to four samples from each size-group were prepared and examined in transmission at seven incidence angles (0°–60°). The center of the selective wavelength band was estimated by visual integration and recorded as λ_r -meas. The wavelength at 0° was recorded as λ_0 . Equation (1) was used to calculate λ_r -theo. When measuring in transmission, the implicit assumption is $\theta_i = \theta_r$. The value of \bar{n}_{ch} is 1.6, based on Abbe refractometer⁵⁶ measurements of the unfractured CLC films by a technique determined earlier for nematic liquid crystal polymers.⁵⁷ Figure 74.80 shows how well the average selective-reflection-wavelength measurements from each size-group agree with the calculated theoretical values.



G4162

Figure 74.80 Angle dependence of selective wavelength reflection as a function of flake size.

The 45- to 90- μm flakes show better agreement with Bragg’s Law in the form of Fergason’s Equation than do the other two size-groups. We attribute this to a better orientation of the medium-sized flakes on the substrate. Their aspect ratio is large enough that the largest dimension is perpendicular to the thickness, so, during the water-bead orientation, the helix axis can align perpendicular to the substrate.

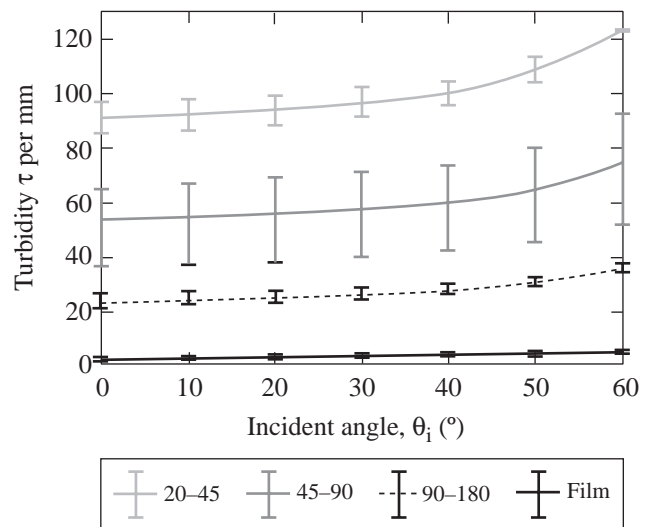
Scattering

We will interpret “scattering” here to refer to any redirection of light from its original path of propagation. As such, use of turbidity as a measure of scattering simply compares transmit-

tance of samples, where lower transmittance corresponds to greater scattering. This section will show that the primary source of scattering by CLC flakes is the misalignment of the helix axes of individual flakes with respect to the substrate.

The same CLC670 samples prepared for angle-dependent wavelength studies were used for turbidity calculations. Turbidity was measured with a horizontal-pass HN32 Polaroid polarizing film⁵⁸ in the spectrophotometer as part of the background correction protocol. As incident angle was increased, the incident polarization remained *P*-polarized. The wavelength chosen for turbidity measurements needed to be well outside the selective reflection region, outside the region of substrate or CLC absorptivity, and part of a normal transmission scan that would not involve lamp, detector, or other voltage-dependent instrument changes; therefore, the chosen measurement wavelength was 900 nm.

The %T of a “blank” sample, i.e., a sample with everything but the liquid crystal, as well as the %T of the sample *with* liquid crystal were recorded at the same incident angle. Turbidity was calculated for all samples using Eq. (3) and averaged within each size-group at each incidence angle. Figure 74.81 shows the turbidity ranges of multiple samples of each group as well as for an unfractured continuous film. For each sieved size-group, the turbidity increases as the incident angle increases. The smaller the flakes, the higher the turbidity per unit thickness.



G4163

Figure 74.81 Turbidity ranges of multiple samples of each sieve group of CLC670 flakes.

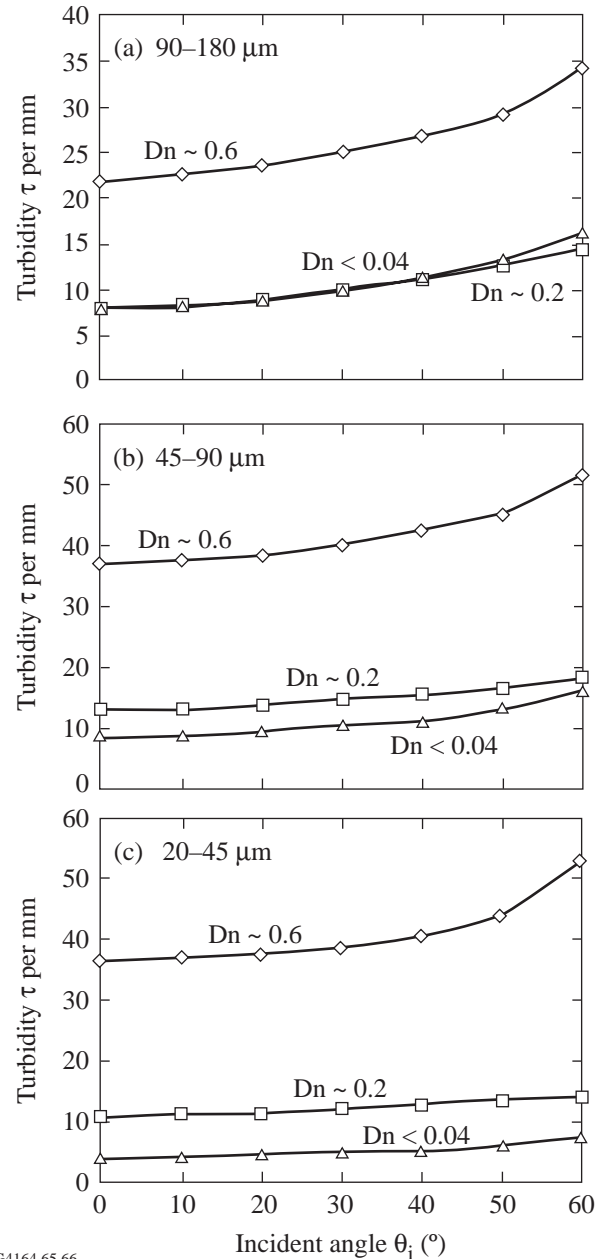
As we saw in Fig. 74.78, transmission scans of flake samples of decreasing median size grow gradually wider and flatter with overall lower-percent transmittance. Due to their small aspect ratio, smaller flakes are not necessarily aligned with their helix axes perpendicular to the substrate. There will, then, be many angles of incidence and reflection for which some wavelength of a spectral scan will meet the Bragg/Ferguson criterion of Eq. (2). Selective reflection may be expected to occur fairly uniformly across the spectrum as the variety of CLC flake orientations increases. As flake sizes get smaller, more flakes are required to cover the same sample area, resulting in this increase in orientation possibilities. Consequently, the turbidity increases as the disorder of the smaller flakes redirects more light out of the original propagation direction.

The flakes are still not small enough to be of the size of the measurement wavelength so we are examining the scattering geometrically. In anticipation of eventually being able to make CLC flakes as small as the domains of the other more common mixed-media systems,⁵⁹ the use of turbidity as a measure of scattering is used in this study even though it was developed originally for the so-called anomalous diffraction regime^{60,61} in which the wavelength is only slightly smaller than the scatterers.

In analogy with mixed-media systems that employ index match or index mismatch to control scattering, the CLC flake samples were overcoated with one of two transparent hosts: (a) a silicone elastomer designated SE2061,⁶² which has an ~ 0.2 index difference, Dn , from the average cholesteric index of CLC670 or (b) a transparent enamel filtered⁶³ from a commercially available paint⁶⁴ with a <0.04 index difference, Dn , from CLC670. In the overcoating process, 1 mL of host in a graduated medicine dropper was added dropwise to the center of the flake sample. Each host flowed uniformly and in its own time to the edge of the sample substrate. The overcoated flake samples were measured in the same way as the others, and turbidity was calculated for seven incident angles.

The turbidities of an uncoated sample, a sample overcoated with the moderate index match (SE2061), and a sample overcoated with the close index match (Testor's Enamel) are plotted for each size-group in Figs. 74.82(a), 74.82(b), and 74.82(c). In every case, overcoating with a host reduces the turbidity of the flake samples. There appears to be less of a difference between a moderate and a good index match than between a coated and an uncoated sample regarding turbidity of the larger flakes. In addition, the overcoated flakes show a

narrower selective reflection band than uncoated flakes,⁶⁵ suggesting that the overcoating process improves the orientation of the flakes. This may explain why there was only a slight difference in turbidity between moderately and nearly index-matched CLC flakes: It is not the index match but rather



G4164,65,66

Figure 74.82

Comparison of turbidities of each flake size-group as a function of index match and incident angle. Each legend indicates the index mismatch of the flakes and host: 0.6 is air, 0.2 is SE2061, and <0.04 is enamel. The flake size-groups shown are (a) 90 to 180 μm , (b) 45 to 90 μm , and (c) 20 to 45 μm .

the flowing action of the hosts that reorients the flakes and reduces scattering.

Applications of Results

CLC flakes as part of a mixed medium can provide three main venues of use: decorative arts, document security, and models of other mixed-media systems. In the realm of decorative arts, we have shown elsewhere⁶⁶ that CLC flakes, with or without a host, can be successfully modeled and measured by standard colorimetric methods. As such, CLC flakes in a suitable host, such as the enamel used in this study, provide versatile paints and inks, which we have applied by brush, airbrush, and fountain pen to surfaces including paper, cloth, metal, and glass.

CLC flakes may also be considered for use in document security. Polymerized CLC films have been suggested for this purpose as overlays.⁶⁷ CLC flakes can be embedded into paper currency, for example, avoiding the problem caused by thin, brittle films. The use of CLC's allows angle-dependent color suitable for first-line identification. The unique polarized-reflection capability of CLC flakes provides a further deterrent to counterfeit reproduction.

Finally, CLC flakes are discrete cholesteric domains, which exhibit none of the limitations of polymer-dispersed and gel systems such as boundary deformations, high-voltage requirements, or domain contamination. With narrower sieve cuts to provide better flake-size uniformity, CLC flakes can provide an excellent physical model of the other mixed-media systems in which the domain is not so clearly characterized. Some work must be done to reduce CLC flake sizes for even closer modeling capability. Toward this end, small quantities of CLC flakes that are only 7 μm thick have been prepared.⁶⁸

Conclusions

We have shown that CLC polysiloxane oligomer films can be fractured into smaller domains called flakes. These CLC flakes can be separated by size and oriented using flotation on an aqueous meniscus. CLC flakes maintain the wavelength and polarization selectivity of the original film. The CLC flakes can also be embedded into an isotropic polymer as a new kind of mixed medium in which the cholesteric domain structure is not contaminated, diluted, voltage dependent, or deformed. As work with this new mixed medium continues, we anticipate that narrower sieve cuts and smaller flakes will allow better use of CLC flakes as models for polymer-dispersed and gel CLC systems.

ACKNOWLEDGMENT

The authors thank Dr. F.-H. Kreuzer and Dr. Robert Maurer of the Consortium für elektrochemische Industrie GmbH and Munich for the CLC polysiloxanes. This work was supported by the U. S. Department of Energy, Office of Inertial Confinement Fusion under Cooperative Agreement DE-FC03-92SF19460, the University of Rochester, and the New York State Energy Research and Development Authority. The support of DOE does not constitute an endorsement by DOE of the views expressed in this article. Funding was also provided by Reveo, Inc.

REFERENCES

1. P. P. Crooker and D. K. Yang, *Appl. Phys. Lett.* **57**, 2529 (1990).
2. R. A. M. Hikmet, *Liq. Cryst.* **9**, 405 (1991).
3. G. S. Chilaya and L. N. Lisetski, *Mol. Cryst. Liq. Cryst.* **140**, 243 (1986).
4. H. L. De Vries, *Acta Cryst.* **4**, 219 (1951).
5. W. U. Müller and H. Stegemeyer, *Berichte der Bunsen-Gesellschaft.* **77**, 20 (1973).
6. F. C. Frank, *Faraday Discuss. Chem. Soc.* **25**, 19 (1958).
7. M. Kléman, *Rep. Prog. Phys.* **52**, 555 (1989).
8. C. M. Dannels and C. Viney, *Polymer News.* **16**, 293 (1991).
9. C. Viney and C. M. Dannels, *Mol. Cryst. Liq. Cryst.* **196**, 133 (1991).
10. L. L. Chapoy, B. Marcher, and K. H. Rasmussen, *Liq. Cryst.* **3**, 1611 (1988).
11. A. Keller *et al.*, *Faraday Discuss. Chem. Soc.* **79**, 186 (1985).
12. M. F. Grandjean, *Comptes Rendus Acad. Sci.* **172**, 71 (1921).
13. R. Cano, *Bull. Soc. fr. Minéral. Cristallogr.* **92**, 20 (1968).
14. P. Kassubek and G. Meier, in *Liquid Crystals 2: Proceedings of the 2nd International Liquid Crystal Conference*, edited by G. Brown (Gordon and Breach, New York, 1969), pp. 753–762.
15. P. E. Cladis and M. Kléman, *Mol. Cryst. Liq. Cryst.* **16**, 1 (1972).
16. M. J. Costello, S. Meiboom, and M. Sammon, *Phys. Rev. A.* **29**, 2957 (1984).
17. D. W. Berreman *et al.*, *Phys. Rev. Lett.* **57**, 1737 (1986).
18. F. Livolant and Y. Bouligand, *Mol. Cryst. Liq. Cryst.* **166**, 91 (1989).
19. J. Voss and B. Voss, *Z. Naturforsch.* **31a**, 1661 (1976).
20. P. G. deGennes, *The Physics of Liquid Crystals*, 1st ed. (Clarendon Press, Oxford, 1974), p. 272.
21. I. Heynderickx, D. J. Broer, and Y. Tervoort-Engelen, *Liq. Cryst.* **15**, 745 (1993).

22. G. Binnig, C. F. Quate, and Ch. Gerber, *Phys. Rev. Lett.* **56**, 930 (1986).
23. R. M. Overney *et al.*, *Langmuir* **9**, 341 (1993).
24. H. Yamada, S. Akamine, and C. F. Quate, *Ultramicroscopy* **42–44**, 1044 (1992).
25. H. Finkelmann and G. Rehage, *Makromol. Chem., Rapid Commun.* **1**, 31 (1980).
26. F.-H. Kreuzer *et al.*, *Mol. Cryst. Liq. Cryst.* **199**, 345 (1991).
27. T. J. Bunning *et al.*, *Liq. Cryst.* **16**, 769 (1994).
28. T. J. Bunning *et al.*, Materials Directorate, Wright Laboratory, Wright-Patterson Air Force Base, OH, Interim Report #WL-TR-91-4089 (July 1989–June 1991).
29. C. Viney, G. R. Mitchell, and A. H. Windle, *Mol. Cryst. Liq. Cryst.* **129**, 75 (1985).
30. T. J. Bunning *et al.*, *Mol. Cryst. Liq. Cryst.* **231**, 163 (1993).
31. T. J. Bunning *et al.*, *Liq. Cryst.* **10**, 445 (1991).
32. J. L. Fergason, in *1985 SID International Symposium, Digest of Technical Papers*, edited by J. Morreale (Pallisades Inst. Res. Services, New York, 1985), pp. 68–70.
33. J. W. Doane *et al.*, *Appl. Phys. Lett.* **48**, 269 (1986).
34. M. Radian-Guenebaud and P. Sixou, *Mol. Cryst. Liq. Cryst.* **220**, 53 (1992).
35. D. K. Yang and P. P. Crooker, *Liq. Cryst.* **9**, 245 (1991).
36. S. M. Faris, U.S. Patent No. 5,364,557 (15 November 1994).
37. J. L. Fergason, *Mol. Cryst.* **1**, 293 (1966).
38. P. S. Drzaic and A. M. Gonzales, *Appl. Phys. Lett.* **62**, 1332 (1993).
39. F. Kreuzer, Wacker-Chemie, Consortium für Elektrochemische Industrie GmbH, Zielstattstrasse 20, D-81379 München, Germany.
40. The photoinitiator used is Irgacure-907, the trade name for 2-methyl-1-[4 methyl thiophenyl]2 morpholino propanone-1. Ciba Additives, Ciba-Geigy Corporation, Hawthorne, NY 10532-2188.
41. Silicon Epiprime, 100-mm-diam wafers, WaferNet, Inc., San Jose, CA 95131.
42. Dataplate digital hotplate/stirrer, PMC Industries, Inc., San Diego, CA 92121.
43. Ultra-Precision Glass Fibers, EM Industries, Inc., Advanced Chemical Division, Hawthorne, NY 10532.
44. UV Lamp Model B-100AP and Blak-Ray Ultraviolet Meter Model J-221, UVP, Inc., San Gabriel, CA 91778.
45. Photo used as October image in the American Institute of Physics 1996 “Beauty of Physics” calendar, Photographer: E. M. Korenic, Laboratory for Laser Energetics, University of Rochester, Rochester, NY 14623-1299.
46. In cooperation with Brian McIntyre, Scanning Electron Microscopist, The Institute of Optics, University of Rochester, Rochester, NY 14627.
47. Devcon® 5 Minute® Epoxy, ITW Devcon, Illinois Tool Works Company, Danvers, MA 01923.
48. Digital Instruments Nanoscope® III Scanning Probe Microscope, Digital Instruments, Inc., Santa Barbara, CA 93117.
49. R. Meister *et al.*, *Phys. Rev. E* **54**, 3771 (1996).
50. Newark Wire Cloth Company, Newark, NJ 07104.
51. LA-900 Laser Scattering Particle Size Distribution Analyzer, Horiba Instruments, Inc., Irvine, CA 92714.
52. T. Allen, in *Pigments—An Introduction to Their Physical Chemistry*, edited by D. W. Patterson (Elsevier, Amsterdam, 1967), Chap. 6, pp. 102–133.
53. M. Pohl, Horiba Instruments, Inc., Irvine, CA (private communication) (1994).
54. Digimatic indicator IDC Series 543, Mitutoyo Corporation, Paramus, NJ 07652.
55. Perkin-Elmer Model Lambda-9 spectrophotometer, Perkin-Elmer Corporation, Norwalk, CT 06859-0012.
56. Bellingham and Stanley Model 60/HR Abbe Refractometer, Bellingham and Stanley Ltd., North Farm Industrial Estate, Tunbridge Wells, Kent TN2 3EY, England.
57. E. M. Korenic, S. D. Jacobs, J. K. Houghton, A. Schmid, and F. Kreuzer, *Appl. Opt.* **33**, 1889 (1994).
58. HN32 Polaroid® linear polarizing film, Polaroid®, Polarizing Division, Norwood, MA 02062.
59. G. P. Montgomery, Jr., J. L. West, and W. Tamura-Lis, *J. Appl. Phys.* **69**, 1605 (1991).
60. S. Zumer, *Phys. Rev. A* **37**, 4006 (1988).
61. P. S. Drzaic, *Mol. Cryst. Liq. Cryst.* **261**, 383 (1995).
62. Petrarch Systems, Inc., Bristol, PA 19007.
63. Millex®-FG13 Filter Unit, 0.2 μm , Millipore Corporation, Bedford, MA 01730.
64. Testor’s Gloss Enamel Gold (#1144), The Testor’s Corporation, Rockford, IL 61104.

65. E. M. Korenic, "Colorimetry of Cholesteric Liquid Crystals," Ph.D. thesis, The Institute of Optics, University of Rochester, 1997, pp. 216–219.
66. E. M. Korenic, "Colorimetry of Cholesteric Liquid Crystals," Ph.D. thesis, The Institute of Optics, University of Rochester, 1997.
67. R. L. van Renesse, in *Optical Document Security*, edited by R. L. van Renesse (Artech House, Boston, 1994), Chap. 13, pp. 263–280.
68. S. D. Jacobs and T. Pfuntner, Laboratory for Laser Energetics, University of Rochester, Rochester, NY 14623-1299 (private communication) (1995).

